

A COMPARISON OF BURNING CHARACTERISTICS OF ISO-OCTANE AND ETHANOL FUELS IN AN OPTICAL SI ENGINE

Ben Moxey, Alasdair Cairns, Hua Zhao

Brunel University
Department of Mechanical Engineering
Uxbridge, UB8 3PH, United Kingdom
tel.: +44 1895 274000, fax: +44 1895 232806
e-mail: ben.moxey@brunel.ac.uk

Abstract

Over the next few decades the automotive industry will be faced with a number of challenging decisions as the world's supply of oil reduces and the global population increases beyond 7 billion. These factors have driven some researchers to look at blending fossil fuels with alternatives such as crop-produced alcohols (or so-called biofuels). The currently reported study was concerned with the combustion characteristics of ethanol-iso-octane blended fuels in a specially designed, single cylinder, spark ignition research engine equipped with full bore overhead optical access. The testing was undertaken using port fuel injection (PFI) and was focused on the behaviour of differing ethanol concentrations under varied internal exhaust gas re-circulation levels (IEGR). Simultaneous high speed imaging and in-cylinder pressure data analysis was used to understand the fundamental influence of varying ethanol content on turbulent flame propagation and subsequent mass burning. The resulting images were analysed looking at the speed of the advancing flame and the shape factor of the burning velocity. The initial evidence suggested that under the moderate speeds and loads tested, poor charge mixture preparation associated with ethanol was leading to fast but unstable burn rates. This could be avoided and combustion improved by using increased valve overlap settings, with the hot residuals entering the intake port aiding the full evaporation of the fuel.

Keywords: ethanol, natural light imaging, iso-octane

1. Introduction

For many there are two main drivers behind the desire for using alcohol fuels in internal combustion engines. One: to negate the damages caused by the products of burning carbon-based fossil fuels and two: to seek energy security. With the former, many governments are looking to reduce levels to that of a specific touchstone – for example, several EU countries have sought to reduce their emissions to 80% of those emitted in 2008 by the year 2050 as part of the Kyoto Protocol. Alcohol fuels are seen as a vital additive in this decarbonisation of the fuel source. While it may be a struggle to use alcohol as a 100% replacement for gasoline without several major alterations to the drivetrain, it has been shown that even a minimal blend of ethanol and gasoline can improve NO_x and HC emissions (though there may or may not be a slight CO rise – data has proved inconclusive on this) [5, 7, 8].

With regards to energy security Hedegaard [3] stated in 2007, that payments worldwide to the 13 OPEC nations totalled USD \$1·10¹². These countries included Saudi Arabia, Angola, Iran and Iraq; some of the most hostile and fractious countries in the world. For many “Western” governments to be paying this amount of money to countries of this nature is seen by the public as an insecure transaction. Looking longer-term, many experts see oil as a depletable commodity which will run out within humanity's lifetime. Indeed, the UK government has discussed implementing a fuel rationing strategy from 2020 if the current rate of consumption continues [2]. Pearson [6] has estimated that an additional 64 million extra barrels of oil per day will be required by 2030 to meet the growth in demand from new emerging markets – this extra yearly requirement is just shy of the current total oil reserves in Saudi Arabia (the second largest producer of oil).

Of the types of alcohol fuels available to be implemented directly, and with the greatest ease, into the fuel source ethanol seems the best poised. Compared to gasoline and iso-octane it has a much lower C:H ratio thus reducing carbon output, it has a higher octane number and a much higher auto-ignition limit. The GHG (greenhouse gas) emission reductions are touted as between 19% and 52% depending on methods of production. Ethanol also contains ~35% oxygen which improves the combustion quality and has been shown to help ‘clean’ an engine by flushing deposits from the fuel line.

Ethanol is already in use around the world both in FFVs (Flex fuel vehicles) and bio-fuel cars; with countries like the US, Canada, Sweden and Brazil all selling E85. As for the main market, the USA’s EPA implemented the Clean Air Act in 1970 which mandated that 7.5% of the forecourt gasoline must be ethanol (corn-produced). Brazil has had a similar scheme in place which uses excess sugar production to make PRO-ALCOOL containing ~22% ethanol. This practice of biofuel addition has since spread to the rest of the world with most of Europe adding up to 5% and Australia up to 10%.

The most touted benefit of ethanol combustion is the lower flame temperature and luminosity, meaning that less heat is lost via radiation and conduction, and the faster burn rates, which can provide a higher BMEP and better torque development. The aim of this work is to investigate the truth in this and to what scale ethanol is faster than a baseline fuel.

2. Experimental engine facilities

The engine used for this work is a Lister Petter TS-1 coupled to a bespoke cylinder head to allow for the full-bore optical access required to give full view of the spark kernel. It is a single, 633 ccm cylinder with a bore of 95 mm and a stroke of 89 mm. Full details of the engine geometry is given in Tab. 1. A diagram of the head is provided in Fig. 1.

An engine speed of 1500 RPM was used throughout the experiments. Fuel was injected into the intake manifold via a Bosch EV6 PFI. This was set at such an angle and location so as to fully coat the back of the intake valves with vaporised fuel. With 25° valve overlap there is thought to be a considerable amount of IEGR retained in the cylinder upon exhaust valve closing (EVC) (up to 10%) and the chance for backflow is high.

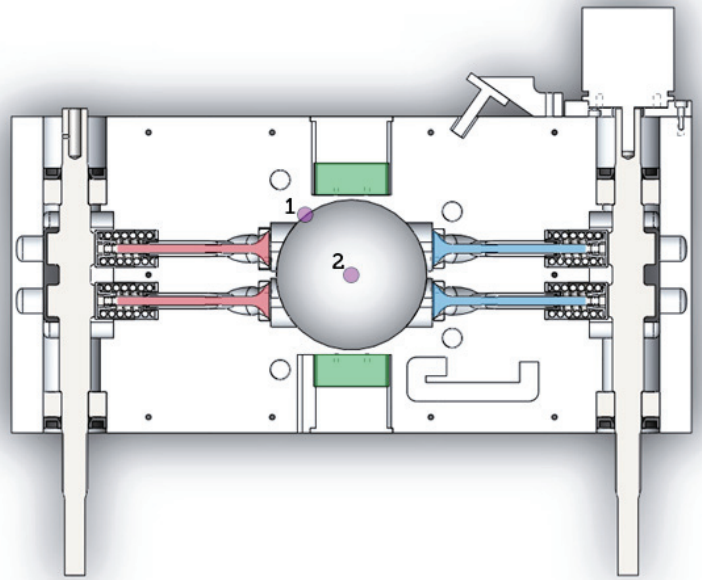


Fig. 1. Overhead view of the redesigned Lister head with the inlet valves shown in blue (right), the exhaust valves shown in red (left), the side windows in green (top and bottom of bore) and the alternative spark locations (1: side and 2: central) as purple discs

Tab. 1. Engine specification

Bore (mm)	95
Stroke (mm)	89
Swept Volume (cc)	633
Clearance Height (mm)	14.1
Compression Ratio	8.4
Exhaust MOP ($^{\circ}$ bTDC)	105
Exhaust Valve Lift (mm)	5
Valve Overlap (deg CA)	25
Inlet MOP ($^{\circ}$ aTDC)	100
Inlet Valve Lift (mm)	5
Cylinder Head Window Material	Corning 7890 HPFS Fused Silica

The in-cylinder pressure data was captured via an AVL GH14DK piezo-electric pressure sensor connected to an AVL Flexifem Noise charge amplifier. The data was recorded in 100 consecutive cycle sets at 1° CA intervals by in-house software. This process was repeated until 300 cycles had been obtained so as to reduce the effect of cyclic variation. The intake manifold pressure was logged by a GEMS 1200 pressure transducer. Lambda was determined by an ETAS LSU 4.9 Lambda sensor connected to an ETAS LA4 Lambda meter, this was also logged by the DAQ. In addition to these the temperature in the head, exhaust bridge, intake manifold and oil sump were logged.

By observing not only the rate of the flame's propagation, but also its structure and burn dynamics, the effect of a change in fuel compound can be determined. Some fuels may induce more turbulence which would be apparent not only from the slow burn speeds but also from visual confirmation that the flame front is more 'wrinkled' and distorted as the charge motion is disturbed in its progress across the bore.

3. Optical imaging techniques

An NAC MEMRECAM fx 6000 high speed video camera coupled to a DRS Hadland Model ILS3-11 image intensifier was used to record all optical data for this experiment. The camera was triggered at the same time as the DAQ to record images simultaneously with the pressure and temperature data. The camera was set to record at 8000 frames per second (fps) at a resolution of 512×308 pixels meaning that the time-resolved images acquired would be at 1.15 crank angles per image.

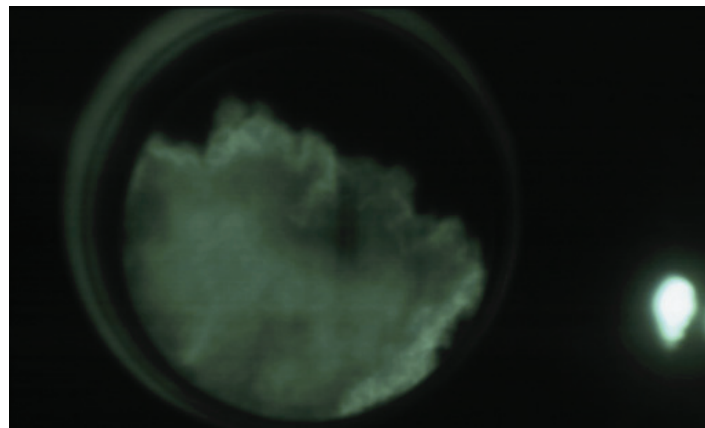


Fig. 2. Graphic detailing a standard image captured during combustion. The bore is evident from the 'halo' of light around it with the propagating flame clear in the centre. The burst of light on the right-hand side is to indicate TDC

In the engine cell the optical equipment was attached to a breadboard, situated over the dynamometer. A mirror positioned at 45° over the bore allowed the camera to capture the images using only the natural light emitted from combustion. While 300 thermodynamic results were obtained with each run, only 50 optical cycles were obtained. This is due to the inherent time-consuming nature of imaging process though percentage variance results have shown that 50 cycles will still provide valid and substantial results.

Once the combustion cycles were captured as a concurrent set of images, they were downloaded as TIFF files with each image representing $125 \mu\text{s}$. In-house software would then batch process the files to convert each TIFF to a black and white image, a mask applied to remove any 'halo' on the bore and finally the image is inverted into black on white with a border circle applied. These stages are laid out in Fig. 3.



Fig. 3. Different stages of image processing

The software also provided the user with an Excel file of the flame radius for each image as it propagated through the cylinder. This radius calculation was performed by assuming the propagating flame is an overlapping, expanding circle with its centre at the spark plug location. By calculating the area bounded between the bore and the new theoretical circle, a calculated radius was provided for each image and from this a flame speed between images.

4. Fuels

A list of the two fuels to used in this study is shown in Tab. 2. Of interest and of note for this experiment is the higher heat of vaporisation and the lower stoichiometric air-fuel ratio which allow for better engine performance by increasing the mass of fuel inducted into the cylinder though this, superficially, will have a hugely detrimental effect on the fuel economy.

Tab. 2. Some of the fuel properties for comparison

Property	Iso-Octane	Ethanol
Chemical Formula	C_8H_{18}	$\text{C}_2\text{H}_5\text{OH}$
Density at P_{atm} and T_{atm} (kg/l)	0.69	0.79
Lower Heating Value (MJ/kg)	44.3	26.8
Stoichiometric AFR	15.1	9
RON	100	109
Latent Heat of Vaporisation (kJ/kg)	270	930
Oxygen Content by Weight (%)	0	34.8

This engine is running a PFI. Some authors in the past have experienced issues with vaporisation, citing that the extra energy required to elevate the port-injected liquid fuel to a vapour is detrimental to the charge temperature. Kar [4], for one, stated that most of the fuel heating was performed by the wall transfer but, as he ran heated inlet air, it is impossible to ascertain where the vaporising

energy actually came from. It is thought that by shifting to a direct injector (DI) this issue can be averted, as shown by Aleiferis [1]. A DI is run at much higher pressures, therefore guaranteeing the vaporisation of the fuel.

5. Thermodynamic results

As already discussed, one of the biggest benefits of using ethanol is its faster burn rate; while this can be identified via optical means, it would be prudent to obtain thermodynamic data to confirm initial thoughts. All experimental data was obtained at 1500 RPM with stoichiometric fuelling and MBT spark timing for each fuel.

Figure 4a demonstrates the rate of heat release from the two fuels when calculated using the Wiebe function. Ethanol has a spark timing of 24° bTDC, some 5° retarded from the iso-octane’s spark timing to achieve MBT timing. Despite this later spark, the burn duration is much quicker than iso-octane (MFB of ‘1’ is reached by 50.5° aTDC compared to 64.5° aTDC) and the rate of heat release is much quicker as can be seen by the gradient of the curve. At the same time, from observing thermocouple data of the cylinder head, the maximum temperature of ethanol combustion is some 2° lower than iso-octane.

Figure 4b shows the IMEP and the co-efficient of variation (COV) of IMEP. Of interest is the COV of IMEP which clearly shows that while ethanol has a faster burning speed, it is a more unstable burn. One suggestion for this may be due to the ~10% residual gas percentage in the cylinder upon EVC. Traditionally, the presence of residual gases in the cylinder would slow down a flame’s burn speed, increasing turbulence and raising the chance of incomplete burns or misfires; all of this would lead to a rise in the COV. However, it appears that the residual gases have little effect on the burn speed of ethanol while still destabilising the burn completion.

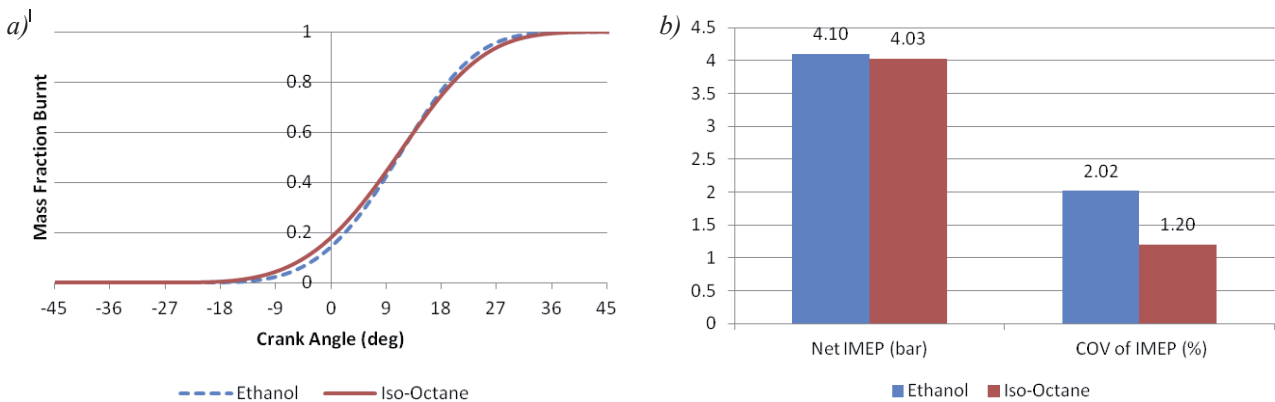


Fig. 4. a) Wiebe function curve and b) IMEP and COV of IMEP

Another suggestion for the curious ethanol combustion is poor charge mixing. As stated earlier, the latent heat of vaporisation for ethanol is nearly three and a half times that of iso-octane and with a PFI being used not a higher pressure DI, the chance of the inducted fuel-air mixture containing liquid fuel or larger droplets is higher for ethanol than iso-octane. This prompted further investigation as to the effect that the overlap was having on the ethanol fuel’s combustion. The EMOP timing was retarded further from TDC to create 30° of overlap and both fuels were run again. When running an extra 5° overlap the COV of iso-octane rose from 1.2% to 2.45%, as would be expected with raised residual levels. However the COV of ethanol halved from 2.02% to 1.1%. With this, the burn duration for the ethanol remained similar while iso-octane took longer to complete burning. This would support the notion that EGR/Residual gas levels have little effect on the duration of the ethanol flame like they would an ordinary fuel, but the increase in residual levels raises the heat of the inducted charge, improving mixing and aiding the stability of the burn.

6. Optical results

In Fig. 5 the results of the optical imaging can be seen. Displayed side-by-side are two strips of images taken at identical crank angles relative to TDC. Also noted is the crank angle after spark for each fuel. This data confirms that seen in the thermodynamic data that even though the spark event for ethanol is 5° after that of iso-octane, its flame expands faster.

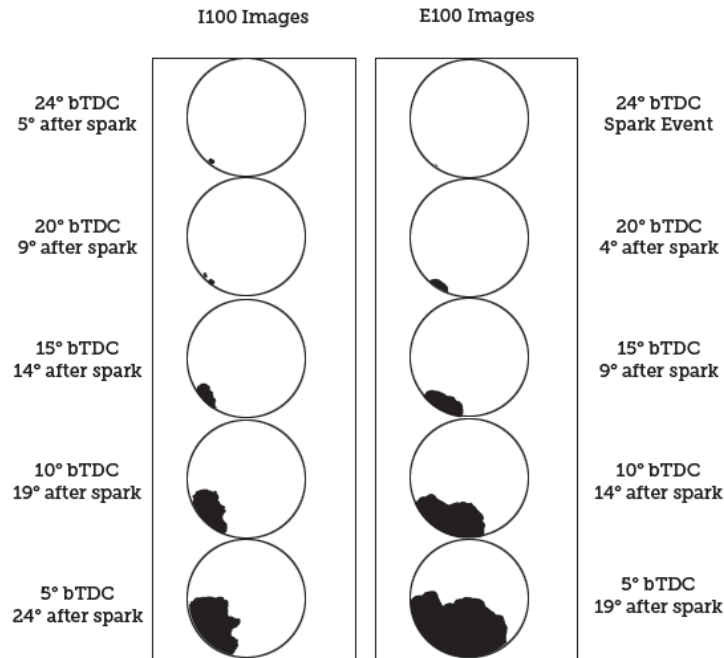


Fig. 5. Side-by-side comparison of the iso-octane (I100) and ethanol (E100) images captured

In Fig. 6 the mean flame speeds are shown. These are calculated from each of the flame images throughout the cycle, averaged for the 50 cycles captured. From this it can be seen that the burn speed patterns appear quite similar in profile but that ethanol has a much higher speed from 18° bTDC. At its peak, the ethanol flame speed is 35.43 m/s, about 10 m/s faster than iso-octane.

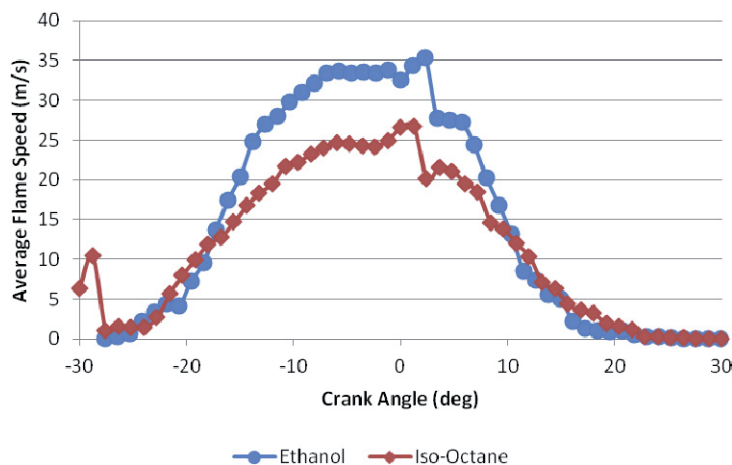


Fig. 6. Flame speed traces for both ethanol and iso-octane fuels

7. Conclusions

The flame speeds of both neat ethanol and iso-octane were tested in a single-cylinder, full-bore optical engine at 1500 RPM with PFI. The two fuels were analysed over 300 cycles for thermo-

dynamic data and 50 cycles for optical data to give a smoothed average figure. All tests were carried out at MBT spark timing and stoichiometric fuelling. The conclusions of the study are summarised as follows:

- from both the thermodynamic and the optical data demonstrates that ethanol possesses a higher P_{max} than iso-octane, which is most likely due to the higher flame speeds experienced. It could also be related to the oxygen content that the alcoholic hydroxyl element provides, allowing for a better burn quality,
- the rate of heat release for ethanol is much quicker than that of iso-octane. This aligns with the publicised fact that ethanol has faster burn rates. It is key to point out that even though the heat release *rate* for ethanol is quicker, the heat release *peak* was much lower for ethanol, proving that ethanol has a much lower burn temperature,
- the COV of IMEP for ethanol is much higher than that of iso-octane. This demonstrates that although the burn speed is higher, the completion of burn and the power output of the ethanol results are varied. This would imply that the residual gases in the cylinder have the effect of destabilising the burn outcome but don't seem to retard the speed as ethanol's burn speed is still far beyond that of initial assumptions.

Further work must be carried out to investigate the effect of the conditions on ethanol's burn speed and completion rates. Due to the higher value of the vaporisation requirement for ethanol, an ambient temperature manifold may be inducting liquid fuel. A study should be carried out looking at the effect of inlet air heating and variable valve overlap on the burn speeds. The expectation is that as the valve overlap increases, the rising residual levels will slow the burn rate and increase the COV but initial experiments have cast doubt on whether ethanol fuel will follow this trend.

References

- [1] Aleiferis, P. G., et al., *An Optical Study of Spray Development and Combustion of Ethanol, Iso-Octane and Gasoline Blends in a DISI Engine*, SAE Paper 2008-01-0073, 2008.
- [2] Fleming, D., Chamberlin, S., *Tradable Energy Quotas: A Policy Framework for Peak Oil and Climate Change*, London: All-Party Parliamentary Group on Peak Oil, and The Lean Economy Connection, 2011.
- [3] Hedegaard, C., Available: <http://news.bbc.co.uk/1/hi/programmes/hardtalk/7654563.stm>, 2008, last accessed 08/06/2012.
- [4] Kar, K., et al., *Measurement of Vapor Pressures and Enthalpies of the Vaporisation of Gasoline and Ethanol Blends and Their Effects on Mixture Preparation in an SI Engine*, SAE Paper 2008-01-0317, 2008.
- [5] Karman, D., *Ethanol Fuelled Motor Vehicle Emissions: A Literature Review*, Air Health Effects Division, Health Canada 2003.
- [6] Pearson, R. J., et al., *Extending the Supply of Alcohol Fuels for Energy Security and Carbon Reduction*, SAE Paper 2009-01-2764, 2009.
- [7] Varde, K. S., Manoharan, N. K., *Charaterization of Exhaust Emissions in an SI Engine Using E85 and Cooled EGR*, SAE Paper 2009-01-1952, 2009.
- [8] Wallner, T., Frazee, R., *Study of Regulated and Non-Regulated Emissions from Combustion of Gasoline, Alcohol Fuels and their Blends in a DI-SI Engine*, SAE Paper 2010-01-1571, 2010.

